EPJ Web of Conferences **107**, 03007 (2016)
DOI: 10.1051/epjconf/201610703007

Collectivity of neutron-rich Cr and Fe toward N=50

V. Werner[1], C. Santamaria[2,3], C. Louchart[1], A. Obertelli[2,3], P. Doornenbal[3], F. Nowacki[4], G. Authelet[2], H. Baba[3], D. Calvet[2], F. Château[2], A. Corsi[2], A. Delbart[2], J.-M. Gheller[2], A. Gillibert[2], T. Isobe[3], V. Lapoux[2], M. Matsushita[5], S. Momiyama[3,6], T. Motobayashi[3], M. Niikura[6], H. Otsu[3], C. Péron[2], A. Peyaud[2], E.C. Pollacco[2], J.-Y. Roussé[2], H. Sakurai[3,6], M. Sasano[3], Y. Shiga[3,7], S. Takeuchi[3], R. Taniuchi[3,6], T. Uesaka[3], H. Wang[3], K. Yoneda[3], F. Browne[8], L.X. Chung[9], Zs. Dombradi[10], S. Franchoo[11], F. Giacoppo[12], A. Gottardo[11], K. Hadynska-Klek[12], Z. Korkulu[10], S. Koyama[3,6], Y. Kubota[3,5], J. Lee[13], M. Lettmann[1], R. Lozeva[4], K. Matsui[3,6], T. Miyazaki[3,6], S. Nishimura[3], L. Olivier[11], S. Ota[5], Z. Patel[14], N. Pietralla[1], E. Sahin[12], C. Shand[14], P.-A. Söderström[3], I. Stefan[11], D. Steppenbeck[5], T. Sumikama[15], D. Suzuki[11], Zs. Vajta[10], J. Wu[3,16], and Z. Xu[13]

[1] *Institut für Kernphysik, Technische Universität Darmstadt, 64289 Darmstadt, Germany*
[2] *CEA, Centre de Saclay, IRFU, F-91191 Gif-sur-Yvette, France*
[3] *RIKEN Nishina Center, 2-1 Hirosawa, Wako, Saitama 351-0198, Japan*
[4] *IPHC, CNRS/IN2P3, Université de Strasbourg, F-67037 Strasbourg, France*
[5] *Center for Nuclear Study, University of Tokyo, RIKEN campus, Wako, Saitama 351-0198, Japan*
[6] *Department of Physics, University of Tokyo, 7-3-1 Hongo, Bunkyo, Tokyo 113-0033, Japan*
[7] *Department of Physics, Rikkyo University, 3-34-1 Nishi-Ikebukuro, Toshima, Tokyo 172-8501, Japan*
[8] *School of Computing Engineering and Mathematics, University of Brighton, Brighton BN2 4GJ, United Kingdom*
[9] *Institute for Nuclear Science & Technology, VAEI, 179 Hoang Quoc Viet, Cau Giay, Hanoi, Vietnam*
[10] *MTA Atomki, P.O. Box 51, Debrecen H-4001, Hungary*
[11] *Institut de Physique Nucléaire Orsay, IN2P3-CNRS, 91406 Orsay Cedex, France*
[12] *Department of Physics, University of Oslo, N-0316 Oslo, Norway*
[13] *Department of Physics, The University of Hong Kong, Pokfulam, Hong Kong*
[14] *Department of Physics, University of Surrey, Guildford GU2 7XH, United Kingdom*
[15] *Department of Physics, Tohoku University, Sendai 980-8578, Japan*
[16] *State Key Laboratory of Nuclear Physics and Technology, Peking University, Beijing 100871, P.R. China*

Abstract. Within the SEASTAR project at RIKEN-RIBF, ^{66}Cr and ^{70,72}Fe have been produced via proton-knockout reactions, and their first excited 2^+ and 4^+ states have been discovered. The combination of the liquid-hydrogen target and TPC system MINOS has been used in combination with the DALI2 detector array for the first time. A 345 MeV/u ^{238}U beam with a mean intensity of about 12 pnA impinged on a Be target. Fission fragments were separated and identified using the BigRIPS spectrograph, and reaction products were analyzed using the ZeroDegree spectrograph. A plateau of excitation energies, with a small change in the systematic trends past $N = 44$, reveals an extension of the $N = 40$ region of collectivity toward $N = 50$. Hence, the isotopes of interest are located within the $N = 40$ island of inversion. An interpretation of the observed trends is offered through large scale shell model calculations.

1 Introduction

Of central interest in contemporary nuclear structure studies is the evolution of shell structure across the nuclear chart. In-medium nucleon-nucleon interactions may shift the energies of individual, or certain subsets of orbitals, such that new shell gaps may open, or vanish, as occupation numbers vary. Starting from the well-known magic numbers, marking significant shell gaps, such behavior has been found as a function of proton and neutron numbers. For example, the N=20 and N=28 magic numbers have been observed to disappear for neutron-rich nuclei in the region of ^{32}Mg [1–3], giving rise to a so-called island of inversion — that is, a sequential filling of proton or neutron orbitals not in the "normal" order, due to two-particle two-hole (2p-2h) configurations, favored because of quadrupole correlations [4–6].

A commonly used first indicator for the existence of shell gaps, and the evolution of collectivity within major nuclear shells, is the energy of the first excited 2^+ state in even-even nuclei. A sudden rise in the 2^+_1 energy, typically on the order of one or few MeV, gives a strong hint on magicity, whereas 2^+_1 energies drop significantly with the onset of collectivity typically to hundreds of keV for vibrators, to tens of keV for well-deformed rotors. Although the absolute energy scale depends on the overall mass region, and may be influenced by other structural properties (e.g., effects of triaxiality or single magicity), the evolution of the $E(2^+_1)$ over a series of isotopes is often

Article available at http://www.epj-conferences.org or http://dx.doi.org/10.1051/epjconf/201610703007

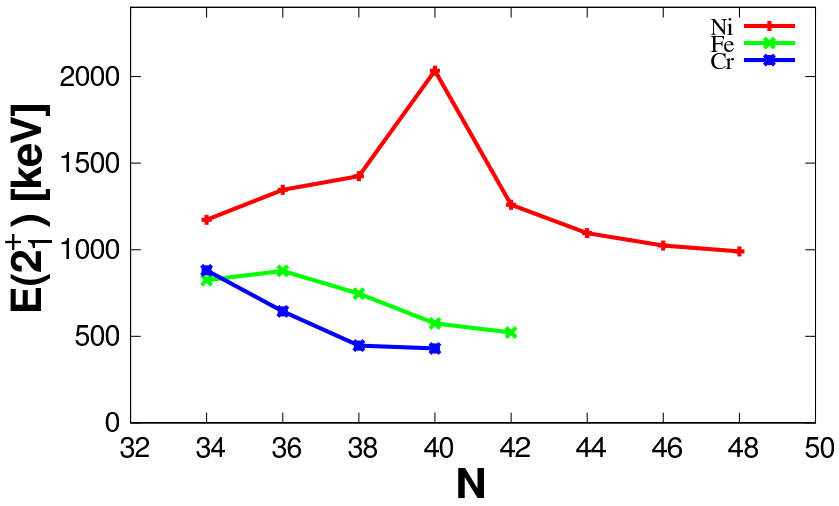

Figure 1. (Color online) Systematics of 2_1^+ energies of even-even Ni, Fe, and Cr isotopes near $N = 40$, as functions of neutron number.

the first indicator for the evolution of structures, and can test or guide nuclear theory. A recent example is the location of a new doubly-magic Ca isotope at $N = 34$ through measurement of its $E(2_1^+)$ values [7] by γ-spectroscopy after proton-knockout at the RIKEN Radioactive Ion Beam Factory (RIBF).

A new project has now been started at RIKEN-RIBF, called "Shell Evolution And Search for Two-plus states At RIBF" (SEASTAR), with the aim of extending our knowledge on the location of 2_1^+ states as far as possible into neutron-rich regions accessible at the RIKEN-RIBF facility. The reach is aided by the novel combination of the DALI2 [8] and MINOS [9] systems, which will be described below, resulting in an excellent experimental sensitivity. Several experiments within the SEASTAR campaigns (first in spring 2014, second in spring 2015) already targeted specific isotopes, or isotopic chains, for which discussions with respect to their underlying shell structure are ongoing. One of these cases addresses the isotopes between $N = 40$–50, below the Ni chain, which will be the topic of this report. In more general, an extension of data into so-far unexplored regions may serve to guide the choice of specific new experiments, where deviations of energy trends from simple model assumptions, hence, potential changes in shell structures, appear.

In the following we will focus on the evolution of collectivity below the $Z = 28$ (Ni) shell closure, specifically on the ^{66}Cr and ^{70,72}Fe isotopes, for which 2_1^+ and 4_1^+ energies are determined for the first time [10].

2 Fe and Cr isotopes with N ≥ 40

Figure 1 shows the existing data on Cr-Ni isotopes in the mass region, where the high 2_1^+ energy in ^{68}Ni marks the closure of the pf neutron shell [11] and suggests a shell gap to the neutron $g_{9/2}$ orbital. However, below the $Z = 28$ shell closure, that is, for Fe and Cr isotopes, no such rise in $E(2_1^+)$ has been observed. In contrast, 2_1^+ energies drop at $N = 40$ in those cases, rather indicating an increase of collectivity than the occurrence of a sub-shell closure when removing only two protons from the $f_{7/2}$ orbital. An increase of collectivity in Fe and Cr isotopes has also been deduced from recent $B(E2)$ measurements [12, 13], which show a modest rise of $B(E2)$ values at $N = 40$. Hence, a new island of inversion has been suggested for the Fe and Cr isotopes at $N = 40$ [14].

This unexpected onset of deformation at N=40 below Z=28 has successfully been reproduced by large-scale shell model calculations [15] within a pf valence space for protons and a $pfgd$ valence space for neutrons, explicitly taking into account the $d_{5/2}$ orbital beyond the N=50 magic shell closure. The term "island of inversion" infers an early filling of higher-lying orbitals, which, within this space, is given through quadrupole correlations between the $1g_{9/2}$ and $2d_{5/2}$ neutron orbitals, leading to the occurrence of particle-hole excitations. In contrast, with missing quadrupole correlations between the pf and the g sub-shells, the ground state of ^{68}Ni is rather uncorrelated [15]. In that case, particle-hole excitations are strong in excited, intruder structures. Similar predictions were made from beyond-mean field calculations based on a collective Hamiltonian [16, 17], where the ^{68}Ni is driven to sphericity by the proton shell closure at $Z = 28$ [16].

Of further interest is the evolution of collectivity toward the $N = 50$ major shell closure and to test its stability below $Z = 28$. Should $N = 50$ disappear, a situation akin to that in the heavier Mg isotopes could be present, with the merger of an island of inversion with a deformed region [3]. The aim of the present work [10], within the first SEASTAR campaign, has been to obtain data on the most neutron-rich accessible members of the Fe and Cr isotopic chains.

3 Apparatus

3.1 Beam production and identification

A primary beam of ^{238}U was provided by the RIBF accelerators, with an energy of 345 MeV/u and an average

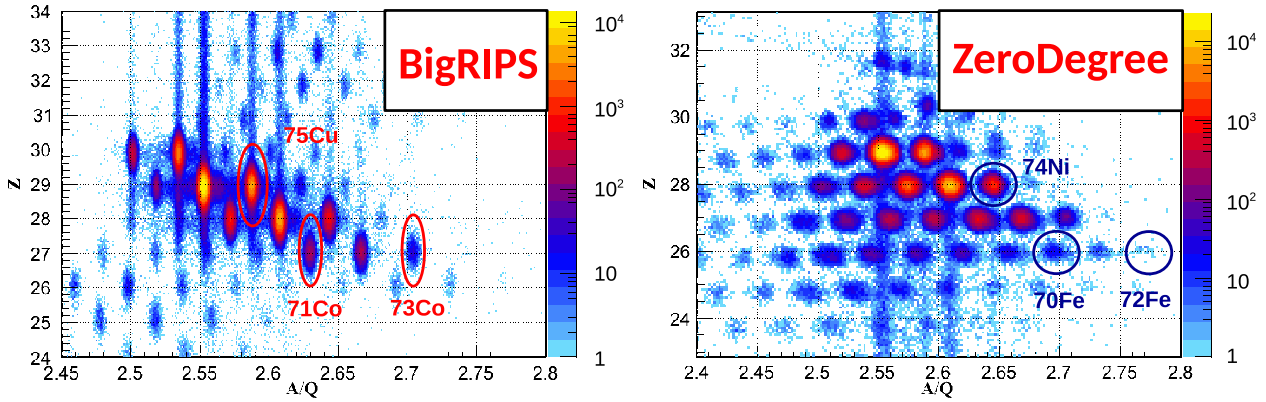

Figure 2. (Color online) Particle identification plots from BigRIPS (left) and the ZDS (right) for the beam setting tuned for Co isotopes. The number of events is color-coded, given as function of Z and mass-over-charge (A/Q).

intensity of 12 pnA. Impinging on a 3-mm thick ^{9}Be primary target, fission fragments were produced at high velocities, and secondary beams of interest were separated out by the BigRIPS separator [18]. Two beam settings were chosen, tuned for ^{67}Mn and ^{71,73}Co, respectively, and secondary beam ions reaching the secondary target were identified through Bρ reconstruction, time of flight and energy-loss measurements in BigRIPS. Therefore, 8-mm and 2-mm thick aluminum wedges were used at two dispersive planes. The total intensities of ^{67}Mn and ^{71,73}Co at the entrance of the secondary target were 12 s^{-1}, 45 s^{-1}, and 6 s^{-1}, respectively, at energies of about 260 MeV/u.

Outgoing reaction residues or unreacted beam were identified by the ZeroDegree spectrometer (ZDS) [19]. As an example, Fig. 2 shows the particle-identification data of BigRIPS and the ZDS from the Co setting. The reaction channel of primary interest was $(p, 2p)$, hence, gates were set on incoming ^{67}Mn and ^{71,73}Co isotopes, which were sufficiently abundant in the beam, and outgoing ^{66}Cr and ^{70,72}Fe isotopes, respectively.

3.2 Target and detection setup

Proton-knockout $(p, 2p)$ reactions occurred on a ^{1}H secondary target of 735(8) mg/cm^2 thickness, which was surrounded by a time projection chamber, both comprising the new MINOS device [9]. MINOS was surrounded by the DALI2 NaI detector array [8] for γ-ray detection, thus, composing the SEASTAR setup for the first time. Further details on the target and detection systems can be found in Ref. [10] and references therein.

The SEASTAR setup led to a luminosity gain of about 3.5 compared to the use of a solid Be target with the same energy loss. In addition, the position information from MINOS allowed to compensate for the Doppler broadening. Since the hydrogen target was extended with a length of 102(1) mm, the MINOS TPC was used not only to select reactions with outgoing protons, but furthermore to reconstruct the reaction vertex by tracking the outgoing protons from the reaction, event-by-event.

The projectile velocity was determined from the reaction vertex, assuming a linear stopping within the hydrogen target. The efficiency for detection and reconstruction of one or two protons was 95 %, and a vertex position resolution along the beam axis better than 5 mm was achieved [20]. With this spatial resolution the Doppler broadening of γ-rays from the uncertainty in the location of an event approximately matched the Doppler broadening due to solid angle of the DALI2 detectors.

The DALI2 array was composed of 186 NaI detectors, covering an angular range from 7 to 115 degrees with respect to the beam axis. The γ-ray detection efficiency was estimated to be 20 % at 1 MeV, and energy calibrations were performed using standard sources. In order to restore events where the γ-ray scattered between DALI2 detectors, an addback procedure was performed for γ-ray energies greater than 200 keV.

Gates on the high-statistics ^{69}Co$(p, 2p)^{68}$Fe and ^{75}Cu$(p, 2p)^{74}$Ni reactions served for calibrating the systems, e.g., for Doppler reconstruction.

4 Results

The obtained γ-ray spectra from ^{66}Cr and ^{70,72}Fe have been binned to 20 keV/channel and the optimum addback conditions have been determined. Figure 3 shows a sample spectrum from the analysis of ^{70}Fe. At least one proton was required to be detected in MINOS. In case that only one proton was detected, the vertex was constructed from the proton track and the beam axis. Clearly two peaks from γ-ray transitions are observed. At different levels of statistics this has been the case for all three isotopes of interest.

Enough data was obtained in order to perform a $\gamma\gamma$-coincidence analysis, and the two transitions were found to be mutually coincident in all cases. In order to reduce background, a maximum multiplicity of 4 has been applied to DALI2. Figure 4 shows the resulting total projection of a $\gamma\gamma$ matrix for ^{70}Fe, as well as a projection after gating on the higher-lying transition, clearly leaving a signal at the energy of the lower-lying transition. Random background has been subtracted when setting the gate.

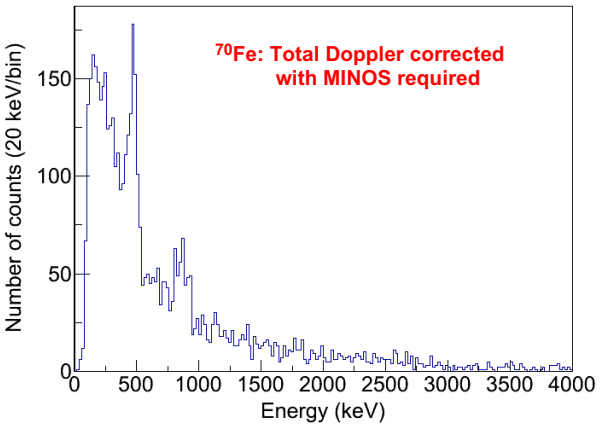

Figure 3. (Color online) Total DALI2 spectrum of ^{70}Fe with addback, but no multiplicity cuts on DALI2 data, and requiring at least one proton to be detected in MINOS.

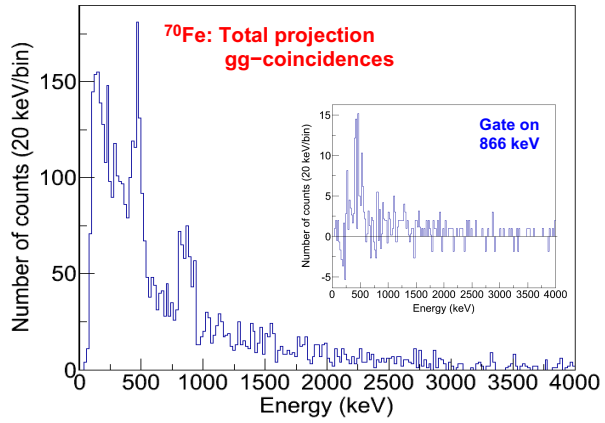

Figure 4. (Color online) Projection of $\gamma\gamma$ coincidences in ^{70}Fe with the same conditions as in Fig. 3, but requiring a maximum multiplicity of 4 in DALI2. The insert shows a projection after a gating condition on the peak at 866 keV.

From these observations and energy systematics, we assign a $2_1^+ \rightarrow 0_1^+$ transition to the lower-lying, more intense, transition in each isotope, and a $4_1^+ \rightarrow 2_1^+$ transition to the respective other, higher-lying transition. Transition energies have been obtained from a fit considering the detector response to the spectra, folding possible lifetime effects into the uncertainty. The procedure can be found in Ref. [10]. Although the spin assignments cannot be made from transition energies only, the made assignment is the most likely with respect to observed intensities, similar observations in other isotopes where the respective states are already known, and the likelihood to populate a $J = 4$ state from knocking a proton out of the $f_{7/2}$ orbital.

Therefore, we assign excited states in ^{66}Cr and ^{70,72}Fe as summarized in Table 1. The results of the final analysis can be found in Ref. [10].

Table 1. Excited state energies assigned in the present work.

^{66}Cr	^{70}Fe	^{72}Fe	
$E(2_1^+)$	386(10) keV	480(13) keV	520(16) keV
$E(4_1^+)$	1069(13) keV	1346(16) keV	1334(20) keV

5 Discussion

The new data extends the energy systematics in the Cr chain up to $N = 42$, and in the Fe chain up to $N = 46$. Since both, the 2_1^+ and 4_1^+ states were observed, we include the ratio $R(4/2) = E(4_1^+)/E(2_1^+)$ in the discussion, which is directly derived from observed transition energies. $R(4/2)$ has limiting values of 2 for spherical harmonic vibrators and 3.33 for well-deformed rigid rotors. Lower values of $R(4/2)$ are typically interpreted as less collectivity, vice versa (see Fig. 3 of Ref. [10]).

The Cr isotopic chain is located in the middle of the proton pf shell and, hence, is expected to display the highest collectivity in the region. The energy of the 2_1^+ state is lowered toward $N = 42$, indicating a further rise of collectivity beyond $N = 40$. An increase of collectivity is also supported by the corresponding rise in the $R(4/2)$ value.

A small, but notable change in the energy systematics in the Fe isotopic chain is observed at $N = 44$, where $E(2_1^+)$ minimizes and $R(4/2)$ maximizes with $R(4/2) = 2.8$, before both values revert their trends. This behavior would typically be interpreted as a signature for maximum collectivity at $N = 44$, and could arise from the filling of the proton $1g_{9/2}$ orbital, which is half-filled at $N = 45$. The valence space for even-even nuclei in such an isolated $g_{9/2}$ shell would be maximized at $N = 44, 46$. In view of previous discussions on extended valence spaces including the $2d_{5/2}$ orbital as in Refs. [15, 16], however, such interpretation seems curious.

In order to obtain a better handle on the underlying microscopic mechanisms leading to the observed trends, shell model calculations were carried out in the same valence space as in Ref. [15]. This valence space comprises the pf proton orbitals, and the $p_{1/2}$, $f_{5/2}$, $g_{9/2}$, and $d_{5/2}$ neutron orbitals. In the LNPS-m interaction used in the present work, minor modifications were applied to the LNPS interaction from Ref. [15], namely on the monopole and pairing parts of the effective Hamiltonian. Calculations using the original LNPS interaction were found to underestimate the 2_1^+ energies of the most neutron-rich isotopes of interest. Therefore, in the LNPS-m interaction, an additional *gd-gd* monopole strength was introduced, leading to stronger intruder configurations in the ground states of these isotopes, and to a better overall agreement between theory and available data in the region. More details on the calculations and their results are shown in Ref. [10], and will be subject of a forthcoming publication.

The modifications to the Hamiltonian do not change the results obtained at $N = 40$ using the original LNPS interaction. The amount of np-nh configurations (up to $n = 6$) is at maximum in the $N = 40$ isotope ^{64}Cr. This indicates that the actual maximum of quadrupole collectivity is found in this isotope, at a maximum deformation

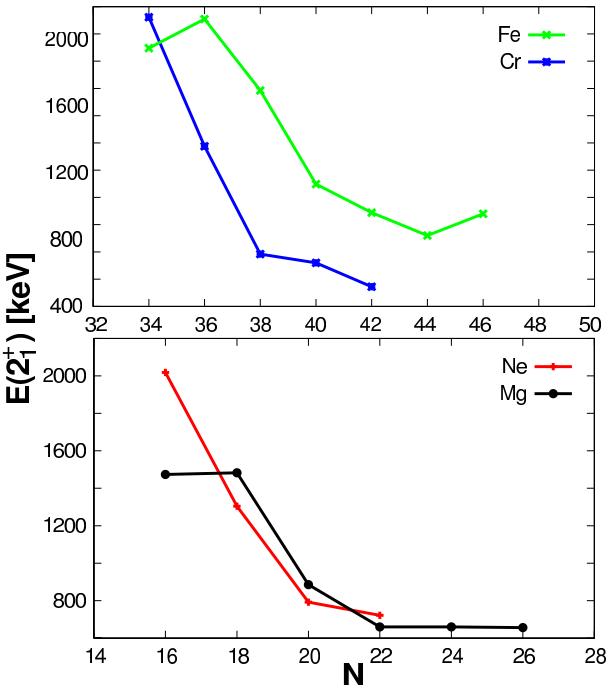

Figure 5. (Color online) Systematics of $E(2_1^+)$ in the Fe and Cr isotopes, across $N = 40$ toward $N = 50$, including the new data (top), and in the Mg and Ne isotopes, across $N = 20$ toward $N = 28$ (bottom).

of $\beta \approx 0.33$. Occupation numbers are found to be similar for states within the ground state band. A similar situation occurs for the Fe isotopes at $N = 40$.

The calculations also yield the largest $B(E2)$ strength and quadrupole moment at $N = 40$, but variations thereafter are rather small. The latter goes along with the down sloping (up sloping), however, near-constant trends of $E(2_1^+)$ ($R(4/2)$) values, which are well-reproduced in the LNPS-m calculation. This seemingly contradicts the conclusions drawn from np-nh configurations indicating the maximum collectivity at $N = 40$. In that case, a stronger peaking of $B(E2)$ strengths and energies could be expected.

Pairing correlations may be one reason for this behavior, which is observed, both, in experiment and calculation. One may consider that, in a simple picture, the first 2^+ state is generated by breaking a pair of nucleons. Should, in addition, the pairing strength be stronger in the 0^+ ground state than in the 2^+ state, the ground-state would be lowered more in energy than the excited state. Hence, the energy difference between both would rise - not due to its quadrupole collectivity.

The pairing expectation values of the multipole Hamiltonian for the ground and first excited states have been extracted from the shell model calculation, and reveal [10] that the minimum in 2_1^+ energies at $N = 44$ is, in fact, due to a smaller pairing correlations difference between the ground state and the 2_1^+ state. Hence, the observed detailed behavior of excitation energies is a consequence of a delicate interplay between quadrupole and pairing correlations.

The revised 2_1^+ energy systematics for the Cr and Fe chains are compared to their counterpart in the Ne and Mg isotopes around $N = 20$, including new data from [3, 21], in Fig. 5. In both cases, a drop of 2_1^+ energies appears where (sub-)shell closures have originally been expected, that is at $N = 40$ and $N = 20$, respectively. Like in the Mg isotopic chain a rather constant behavior of the energies toward the next shell closures, that is $N = 50$ and $N = 28$, respectively, is found. In case of the Mg isotopes, from this trend a quenching of the $N = 28$ shell closure was speculated. This may also be the case for the $N = 50$ shell closure below $Z = 28$.

6 Summary

We have measured the energies of the 2_1^+ and 4_1^+ states of the neutron-rich ^{66}Cr and ^{70,72}Fe isotopes through their γ-ray decays after proton-knockout reactions. In this experiment, we employed for the first time the MINOS device, comprised of a liquid-hydrogen target and a TPC, in conjunction with the DALI2 NaI detector array at the RIKEN-RIBF facility. Although quadrupole collectivity is maximized at $N = 40$, excitation energies vary little beyond $N = 40$, as a consequence of pairing correlations. Within the shell model, this is interpreted as an extension of the $N = 40$ island of inversion toward $N = 50$. However, a test whether this island of inversion actually extends to $N = 50$, which would imply the disappearance of the $N = 50$ shell closure below ^{78}Ni, is not possible to date. In addition, $B(E2)$ values are needed as a more direct test of the collectivity across $N = 40$, and toward $N = 50$.

Acknowledgements

We are grateful to the RIBF and BigRIPS teams for ensuring stable operation and high beam intensities for the primary and secondary beams. The development of MINOS and the core MINOS team have been supported through the ERC Grant MINOS-258567. A. O. acknowledges support through the JSPS long-term fellowship L-13520. C. S. and A.O. are grateful to the RIKEN Nishina Center for its hospitality. L. X. C. has been supported through the LIA program of Vietnam Ministry of Science and Technology (MOST). Z. D. and Zs. V. have been supported by the OTKA K100835 contract. C. L. acknowledges support through HIC for FAIR. Further support was received through BMBF grant 05P12RDFN8, and U.S. DOE grant DE-FG02-91ER-40609.

References

[1] E. Caurier, F. Nowacki, A. Poves, Phys. Rev. C **90**, 014302 (2014)
[2] T. Motobayashi *et al.*, Phys. Lett. B **346**, 9 (1995)
[3] P. Doornenbal *et al.*, Phys. Rev. Lett. **111**, 212502 (2013)
[4] B.H. Wildenthal and W. Chung, Phys. Rev. C **22**, 2260 (1980)
[5] A. Poves and J. Retamosa, Phys. Lett. B **184**, 311 (1987)

[6] E.K. Warburton, J.A. Becker, and B.A. Brown, Phys. Rev. C **41**, 1147 (1990)
[7] D. Steppenbeck *et al.*, Nature **502**, 207 (2013)
[8] S. Takeuchi *et al.*, Nucl. Instr. Meth. A **763**, 596 (2014)
[9] A. Obertelli *et al.*, Eur. Phys. J. A **50**, 8 (2014)
[10] C. Santamaria *et al.*, Phys. Rev. Lett., accepted.
[11] R. Broda *et al.*, Phys. Rev. Lett. **74**, 868 (1995)
[12] W. Rother *et al.*, Phys. Rev. Lett. **106**, 022502 (2011)
[13] H.L. Crawford *et al.*, Phys. Rev. Lett. **110**, 242701 (2013)
[14] J. Ljungvall *et al.*, Phys. Rev. C **81**, 061301 (2010)
[15] S. Lenzi *et al.*, Phys. Rev. C **82**, 054301 (2010)
[16] L. Gaudefroy *et al.*, Phys. Rev. C **80**, 064313 (2009)
[17] K. Sato *et al.*, Phys. Rev. C **86**, 024316 (2012)
[18] T. Kubo *et al.*, Prog. Theor. Exp. Phys. **2012**, 3C003 (2012)
[19] N. Fukuda *et al.*, Nucl. Instr. Meth. B **317**, 323 (2013)
[20] C. Santamaria *et al.*, (in preparation)
[21] P. Doornenbal *et al.*, Phys. Rev. Lett. **103**, 032501 (2009)